

AFWL-TR-81-147

AFWL-TR-
81-147

1

BLEST IMPULSE TIME-OF-FLIGHT SPHERE

H. Gay

New Mexico Engineering Research Institute
University of New Mexico
Albuquerque, NM 87131

May 1982

Final Report

Approved for public release; distribution unlimited.

THIS RESEARCH WAS SPONSORED BY THE DEFENSE NUCLEAR AGENCY UNDER
SUBTASK H53BAXYX, WORK UNIT 0005, WORK UNIT TITLE: "2604 GAGE
EVALUATION."

AIR FORCE WEAPONS LABORATORY
Air Force Systems Command
Kirtland Air Force Base, NM 87117

DTIC
ELECTE
JUL 15 1982
S B D

82 07 15 066

AD A116940

DTIC FILE COPY



AFWL-TR-81-147

This final report was prepared by the New Mexico Engineering Research Institute, Albuquerque, New Mexico, under Contract F29601-81-C-0013, Job Order WDNS0341 with the Air Force Weapons Laboratory, Kirtland Air Force Base, New Mexico. Mr Josef F. Schneider (NTEO) was the Laboratory Project Officer-in-Charge.

When Government drawings, specifications, or other data are used for any purpose other than in connection with a definitely Government-related procurement, the United States Government incurs no responsibility or any obligation whatsoever. The fact that the Government may have formulated or in any way supplied the said drawings, specifications, or other data, is not to be regarded by implication, or otherwise in any manner construed, as licensing the holder, or any other person or corporation; or as conveying any rights or permission to manufacture, use, or sell any patented invention that may in any way be related thereto.

This report has been authored by a contractor of the United States Government. Accordingly, the United States Government retains a nonexclusive, royalty-free license to publish or reproduce the material contained herein, or allow others to do so, for the United States Government purposes.

The Public Affairs Office has reviewed this report, and it is releasable to the National Technical Information Service, where it will be available to the general public, including foreign nationals.

If your address has changed, if you wish to be removed from our mailing list, or if your organization no longer employs the addressee, please notify AFWL/NTEO, Kirtland AFB, NM 87117 to help us maintain a current mailing list.

This report has been reviewed and is approved for publication.


JOSEF F. SCHNEIDER
Project Officer


FRED L. HALLBERG
Major, USAF
Chief, Test Operations Branch

FOR THE COMMANDER


MAYNARD A. PLAMONDON
Chief, Civil Engineering Research
Division

DO NOT RETURN COPIES OF THIS REPORT UNLESS CONTRACTUAL OBLIGATIONS OR NOTICE ON A SPECIFIC DOCUMENT REQUIRES THAT IT BE RETURNED.

UNCLASSIFIED

SECURITY CLASSIFICATION OF THIS PAGE (When Data Entered)

REPORT DOCUMENTATION PAGE		READ INSTRUCTIONS BEFORE COMPLETING FORM
1. REPORT NUMBER AFWL-TR-81-147	2. GOVT ACCESSION NO. AD-A116	3. REPORT'S CATALOG NUMBER 940
4. TITLE (and Subtitle) BLEST IMPULSE TIME-OF-FLIGHT SPHERE	5. TYPE OF REPORT & PERIOD COVERED Final Report	
	6. PERFORMING ORG. REPORT NUMBER NMRI TA10-6	
7. AUTHOR(s) H. Gay	8. CONTRACT OR GRANT NUMBER(s) F29601-81-C-0013	
9. PERFORMING ORGANIZATION NAME AND ADDRESS New Mexico Engineering Research Institute University of New Mexico Albuquerque, NM 87131	10. PROGRAM ELEMENT, PROJECT, TASK AREA & WORK UNIT NUMBERS 62715H/WDNS0341	
11. CONTROLLING OFFICE NAME AND ADDRESS Air Force Weapons Laboratory (NTEO) Kirtland Air Force Base, NM 87117	12. REPORT DATE May 1982	
	13. NUMBER OF PAGES 30	
14. MONITORING AGENCY NAME & ADDRESS (if different from Controlling Office) Director Defense Nuclear Agency Washington, DC 20306	15. SECURITY CLASS. (of this report) Unclassified	
	15a. DECLASSIFICATION/DOWNGRADING SCHEDULE	
16. DISTRIBUTION STATEMENT (of this Report) Approved for public release; distribution unlimited.		
17. DISTRIBUTION STATEMENT (of the abstract entered in Block 20, if different from Report)		
18. SUPPLEMENTARY NOTES This research was sponsored by the Defense Nuclear Agency under Subtask H53BAXYX, Work Unit 0005, Work Unit Title: "2604 Gage Evaluation."		
19. KEY WORDS (Continue on reverse side if necessary and identify by block number) BLEST Time of Flight Velocity Impulse Drag		
20. ABSTRACT (Continue on reverse side if necessary and identify by block number) A time-of-flight sphere was designed, fabricated, and tested to be used to measure impulse delivered by a Berm-Loaded Explosive Simulation Test (BLEST). The timer inside the thin-wall ball was tested for survival by performing drop tests and explosively propelled tests. The takeoff velocity determined from time of flight correlated very closely with the velocity determined by high-speed cameras and photopoles.		

CONTENTS

<u>Section</u>		<u>Page</u>
I	INTRODUCTION	3
II	FABRICATION	5
	Mechanical	5
III	FABRICATION AND OPERATION OF ELECTRONICS	7
	Time-of-Flight Theory of Timer Operation--First Design	7
	Time-of-Flight Theory of Timer Operation--Final Design	7
	Time-of-Flight electronics	8
IV	ASSEMBLY PROCEDURE	11
V	OPERATIONAL SURVIVAL TESTS	13
VI	TIME-OF-FLIGHT AND VELOCITY EQUATIONS	17
VII	CONCLUSION AND RECOMMENDATIONS	23
 <u>Appendix</u>		
A	TIME-OF-FLIGHT AND VELOCITY SAMPLE CALCULATIONS	25

Accession For	
NTIS GRA&I	<input checked="" type="checkbox"/>
DTIC TAB	<input type="checkbox"/>
Unannounced	<input type="checkbox"/>
Justification	
By _____	
Distribution/	
Availability Codes	
Dist	Avail and/or Special
A	



LIST OF ILLUSTRATIONS

<u>Figure</u>		<u>Page</u>
1	Bottom hemisphere	6
2	Top hemisphere	6
3	Backside of watch timer	10
4	Dial of Armitron Chronograph wristwatch	10
5	Sphere assembly	12
6	Launch tube	14
7	Explosively propelled sphere	15
8	Forces acting on vertically launched ball	18
9	Time of flight versus launch velocity with drag	22

LIST OF TABLES

<u>Table</u>		
1	Total impulse as a function of measurement type and zone of the shaped HEST	23
A-1	Time of flight versus launch velocity for earth density spheres	26

I. INTRODUCTION

The objective of this effort was to build and test a gage capable of measuring the specific vertical impulse (peak) imparted by a high-explosive test to the earth or a berm. The specific impulse (I) is defined as the integral of the pressure (P)/time (t) history, or

$$I = \int P \cdot dt$$

Because this pressure is acting on the soil, it forces the soil to move with an acceleration (a) equal to

$$a = \frac{P}{m_A}$$

where m_A is the aerial mass density. Using this relationship, the expression for impulse may be rewritten as

$$I(t) = \int_0^t m_A a \, dt$$

Thus for the case of constant mass density at any time (t_1)

$$I(t) = m_A \left[V(t_1) - V(t_0) \right]$$

where t_0 is some initial time. For the case $V(t_0) = 0$, at any time during the acceleration due to the high-explosive event (neglecting the material strength and assuming a rigid body) the impulse is equal to the momentum of the accelerated body.

This is the principle of a photopole used on high-explosive events. A camera records the photopole's position/time history. The velocity of the berm is then inferred from these data and the impulse may be calculated as a function of time. This technique works quite well for a High Explosive Simulation Technique (HEST) where the overburden is directly above the explosives. However, in the Berm-Loaded Explosive Simulation Technique (BLEST), there are a number of discrete buried charges. The debris from the detonation of these charges quickly obscures any photopole in the test bed.

This inability to measure photopoles mandated the development of something different to measure impulse. The device chosen for this application is the time-of-flight sphere. It, unlike the photopole, is used only to measure peak impulse. The peak impulse (I_p) may be expressed, in the normal case of an initial velocity of zero, as

$$I_p = m_A V_p$$

where V_p is the peak or equilibrium launch velocity in the vertical direction.

The ballistics of a freely launched projectile are well-known. In the first approximation, neglecting air drag*, simple Newtonian mechanics state that a projectile vertically launched in a 1-g downward field will come to rest in a time t_u equal to

$$t_u = \frac{V_p}{g}$$

The projectile will then begin to descend toward the earth and, if it lands at the same elevation it took off from, it will take the same time (t_d) to return, or

$$t_u + t_d = \frac{2V_p}{g} = t$$

where t is the total time of flight. The above equation may be used to obtain an expression for the peak impulse. This is

$$I_p = \frac{m_A g t}{2}$$

The reader should note, as will be shown later, that air drag does affect this result. However, at common BLEST launch velocities the effect is minimal. It is important to note that the relationship is strictly monotonic, i.e., for any increase or decrease in the time of flight, there is a corresponding increase or decrease in the peak impulse. The object of this effort was to establish that relationship for earth density spheres and empirically verify it. Consequently, a method for measuring peak impulse on a BLEST was developed.

*Note: The effect of air drag is calculated in Section VI.

II. FABRICATION

MECHANICAL

The inner container for the time-of-flight timer was fabricated from a 9-cm-diameter steel cylinder 8.5 cm long. One end had a screw-on lid. Six piezoelectric crystals were cemented to the inner container surface and connected to the electronic timer.

The outer container was made up of two spun-aluminum hemispheres having a 15.24-cm radius and a 1.6-mm wall thickness. A 3.5-cm aluminum band was riveted to one hemisphere. The other hemisphere was attached to the band using nut plates and flat socket head 10-32NF screws (Figs. 1 and 2). The top hemisphere had a 25-mm screw-in plug through which sand was poured to fill the space between the inner container and the outer container.

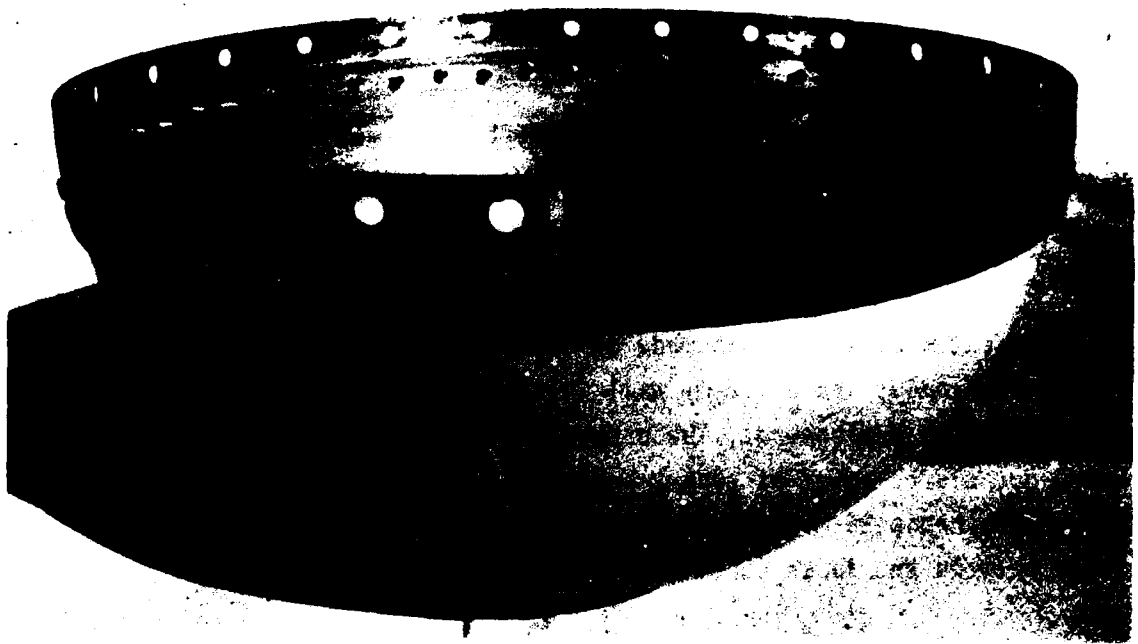


Figure 1. Bottom hemisphere.

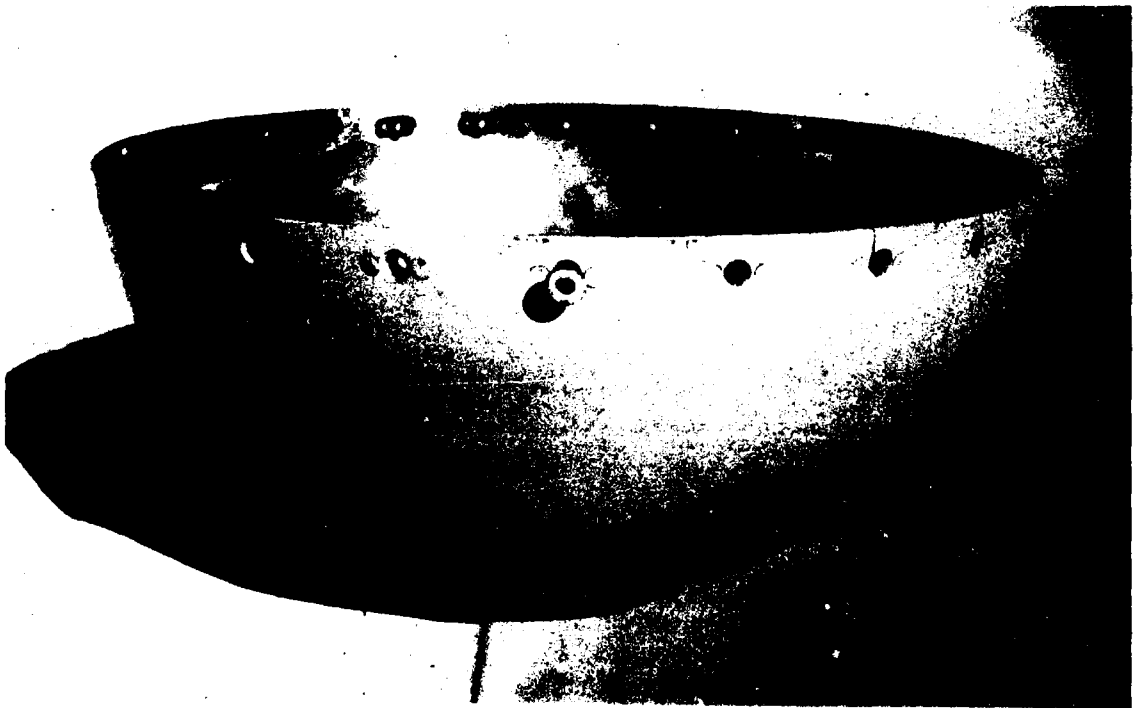


Figure 2. Top hemisphere.

III. FABRICATION AND OPERATION OF ELECTRONICS

TIME-OF-FLIGHT THEORY OF TIMER OPERATION--FIRST DESIGN

The first timer built and tested, unsuccessfully, consisted of a counter card having five integrated circuits and several discrete components. The ICM7215 and its associated oscillator crystal were used to generate all clocking signals. While enabled, the ICM7215 provided an oscillator output of approximately 1 kHz to the 4-stage ripple-carry binary counter/divider (4020). The ICM7215, as wired, was configured to work as a stopwatch. After being reset, the negative-going edge on +START/STOP will start the internal counter, and the second negative-going edge will load the resulting count into display, reset the internal counter, and reinitiate counting. Subsequent negative-going transitions would replace the old count (i.e., the current display) with a new "lap" time, reset the internal counter, and reinitiate counting if it were to occur. The additional support circuitry surrounding the ICM7215 was designed to gate only one start pulse, lock out further pulses on the INPUT line for a period determined by the output selected from 4020, gate only one stop pulse, and lock out all further pulses until a valid RESET occurred. This timer was abandoned after bench tests, drop tests, and explosively propelled tests showed a high failure rate when the display was disconnected and reconnected as is required during drop tests and explosively propelled tests.

TIME-OF-FLIGHT THEORY OF TIMER OPERATION--FINAL DESIGN

The time-of-flight electronics are designed to meet a specific need. A measurement is made of a time increment between acceleration impulses using an Armitron Chronograph wristwatch. The impulses are generated by a positive or negative acceleration in any axis relative to the device. Piezoelectric crystals are used to sense the presence of an acceleration. During a change of acceleration the crystals will displace electrons, which generates a small current. The crystals are arranged in a three-axis sensing orientation utilizing two crystals per axis mounted on opposite sides of the canister. Currents generated by the crystals are fed through a diode OR gate to a voltage comparator. Sensitivity to the acceleration impulses may be adjusted by setting the input level at the differential input of the voltage comparator.

Output from the voltage comparator, signaling an adequate level of impulse, is routed to a flip-flop which is set at that time. Output from the flip-flop is used to accomplish two functions. In the first function, output is sent through an interface transistor to the timer module. Upon receipt of the signal, the timer initiates the counting for the time between impulses. Secondly, output from the flip-flop starts the 1-s lockout time to prevent a false input following the initial pulse. This is accomplished by an RC circuit which is tied to the approximate lockout time necessary. The second acceleration impulse follows the same path through the crystals, the voltage comparator, and to the flip-flops. Upon receipt of the second pulse, the second flip-flop is then set. Output from the second flip-flop is routed through an interface transistor and then to the timer. The second impulse received sets the flip-flop into a set mode and will not allow additional impulses to pass on to the timer. A complete reset procedure must be followed before the module will interpret future impulses. The reset procedure is a five-step operation and is covered under Time-of-Flight Electronics discussed below.

Time-of-flight electronics--Time-of-flight electronics were designed to meet qualifications of withstanding a 1000-g shock environment while resolving the time of flight to 1/100 s. The electronics are wholly contained in two parts. The first part contains the Armitron Chronograph wristwatch timing and interface modules; the second part contains the acceleration-sensitive switch and battery pack. The two parts are interconnected by four wire leads. Both parts are subsequently installed inside a heavy metal can for protection.

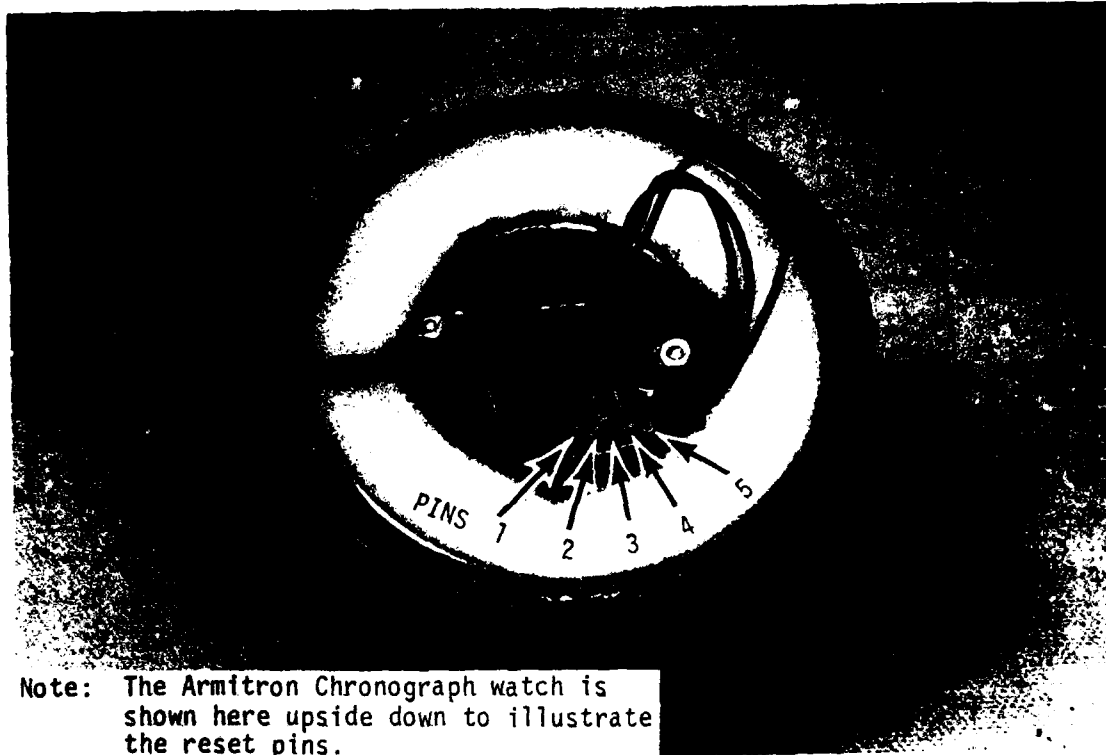
The time-of-flight electronics are designed to be activated by the connection of the five interconnection wire leads. Once activated, the units should be able to operate for approximately 30 consecutive days, or any period cumulative up to the 30-day level, which falls within the one-year storage life of the battery pack. The development of the two-part system allows a new battery pack to be reconnected for reuse of the timing module. The two parts should be connected at a convenient period before use and disconnected before prolonged storage. An accurate time schedule should be kept to determine the battery pack usage and remaining life.

Once the two parts have been connected, the timer must be reset by the recommended reset procedure, covered later in this report, and readied for flight. Flight readiness is achieved when the two parts have been joined, the timer reset, and both have been installed in the canister along with the shock insulating foam pads. The canister is then ready to be installed in the sand-filled sphere. Care should be exercised to prevent shock or high accelerations being imparted to the canister or sphere to prevent premature starts of the timing module. Sensitivity was set for approximately a 50-g threshold to start and stop the timer. This may be translated into a short drop of less than 30 cm onto a hard surface.

The timer is activated due to an acceleration in any axis which is greater than its threshold. The first (initial) pulse will start the timer running. There follows a period of approximately 1 s which is interlocked to the timer and will prevent a second shock pulse from stopping the timer. The next acceleration impulse following the interlock time will stop the timer. The timer will then hold the time between impulses on its display until externally reset. The timer is disabled following the second pulse and will not accept further impulse signals.

To reset the timer, a five-step procedure must be followed. A 30 AWG jumper is inserted into pin 1 and consecutively connected to pin 2, pin 3, pin 4, and pin 5. See Figure 3. At this point the display should read all zeros. If not, the brown wire coming from below the watch face is touched to the pin located at the lower right-hand corner of the watch face and the procedure is repeated. The time-of-flight timer is then ready to measure the time increment within the test environment.

The timer's display consists of two lines. The upper line contains both 1/10-s and 1/100-s increments, while the lower contains 10s and units of minutes, followed by 10s and units of seconds. A typical time of flight would be contained within the last digit of the lower line and the two digits of the upper line of the display. See Figure 4.



Note: The Armitron Chronograph watch is shown here upside down to illustrate the reset pins.

Figure 3. Backside of watch timer.

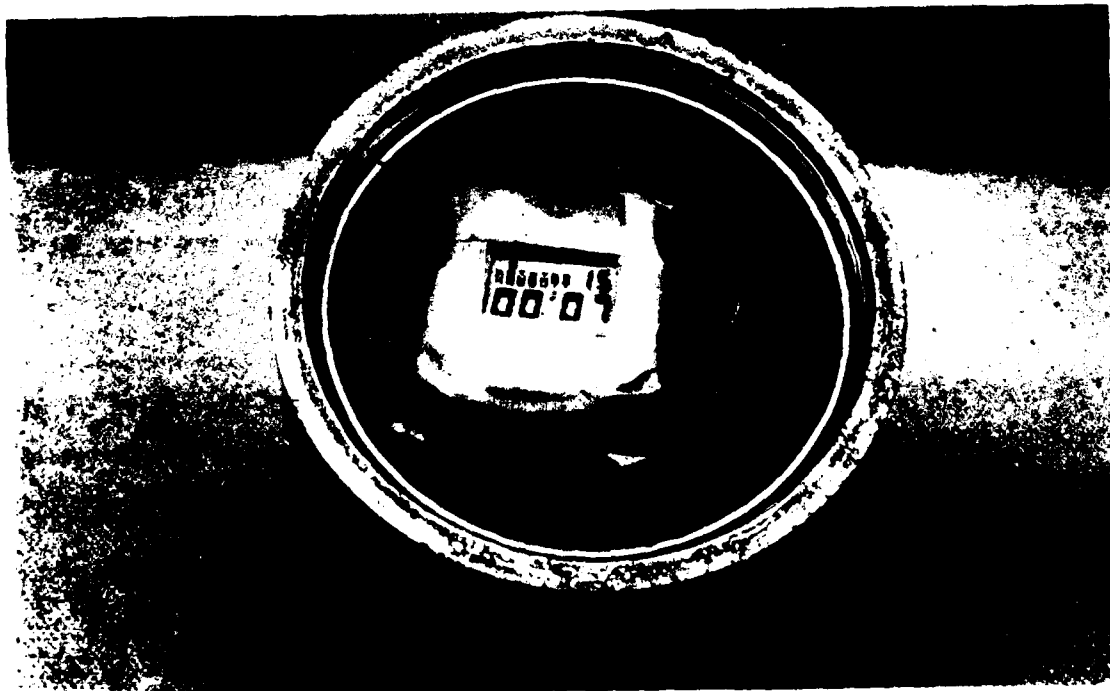


Figure 4. Dial of Armitron Chronograph wristwatch.

IV. ASSEMBLY PROCEDURE

The red wire from the bottom electronics section was cut and taped. Just prior to assembling the time-of-flight sphere, the red wire must be reconnected by soldering or using a twist wire nut and then taped. The timer should be reset prior to field test. To reset the timer, the same five-step procedure discussed previously must be followed. Pin 1 is located at the lower left position when viewing the wristwatch from the rear. There is a black spot under pin 1. A 30 AWG jumper is inserted into pin 1 and consecutively touched to pin 2, pin 3, pin 4, and pin 5. See Figure 3. The display should now read all zeros. The timer is then ready to measure the total time from takeoff to landing. The lower hemisphere, which has the equatorial band riveted in place, should be nearly filled with sand. The inner steel container, which has its timer reset, is placed in the middle of the sand. Next, the top hemisphere is placed inside the equatorial band. The end of the hemisphere opposite the equatorial band split is lowered onto the nut plate, band screw-hole alignment made, and then one 10-32NF screw is installed. Because the band is contoured to the hemisphere radius, the assembly is difficult. The top hemisphere must be worked into the band by prying between band and hemisphere starting at the 10-32NF screw and working each side to the band split. See Figure 5. When the top hemisphere nut plates all line up with the band screw holes, the remaining 24 screws are installed. The top plug is then removed and the remaining top hemisphere cavity is filled with sand and the top filler plug reinstalled.

The assembled spheres are buried to the equator for the field test shots.



Figure 5. Sphere assembly.

V. OPERATIONAL SURVIVAL TESTS

The first timer fabricated consisted of a counter card and a conditioner card connected to eight piezoelectric crystals. All were housed in a steel inner container and an aluminum sphere. Drop tests from the tower of the 2-by 40-ft shock tube were conducted at various elevations from 1 to 13 m; over 50 percent of the tests were failures. The problem was found to stem from the fact that the display unit had to be separated from the timer unit before the drop tests and reconnected after the drop. This same timer was tested for operation and survival by explosively propelling upward the 30-cm-diameter sphere containing the timer. Two explosively propelled tests were performed at a takeoff velocity of 15 m/s and 25 m/s. The timer failed to operate during both tests; therefore, a new timer was fabricated using an Armitron Chronograph wristwatch. With this design, the watch is the display and timer and flies with the sphere as a unit and does not have to be disconnected and separated. This timer system was dropped from a height of 13 m over a hundred times without experiencing any failures. Two of the watch timers were placed in the steel container but not the sand-filled sphere. The steel containers were then placed on top of a berm which explosively propelled the timers upward. Both timers survived and indicated a total flight time of 3.85 s. For the no-drag case, this gives a takeoff velocity of 19 m/s.

After the above tests, two watch timers in two steel containers were placed in one aluminum 30-cm-diameter sphere with the void filled with sand. The sphere was placed inside a 38-cm-i.d. tube 1.2 m long. See Figure 6. The sphere was then explosively propelled upward. A photopole and a 1000-frame/s camera were used to confirm the takeoff velocity derived from the time of flight. See Figure 7. Calculating takeoff velocity from the time of flight for the no-drag case gave 34.7 m/s while the photopole/camera combination indicated that the takeoff velocity was 33.5 m/s. The error between the two time-of-flight methods was 3.33 percent.

The worst error in determining takeoff velocity using the camera/photopole is calculated as follows:

Each photopole alternate black and white stripe was 50.8 mm (2 in) wide. Each frame of the 1000 frame/s camera covered one stripe due to the distance

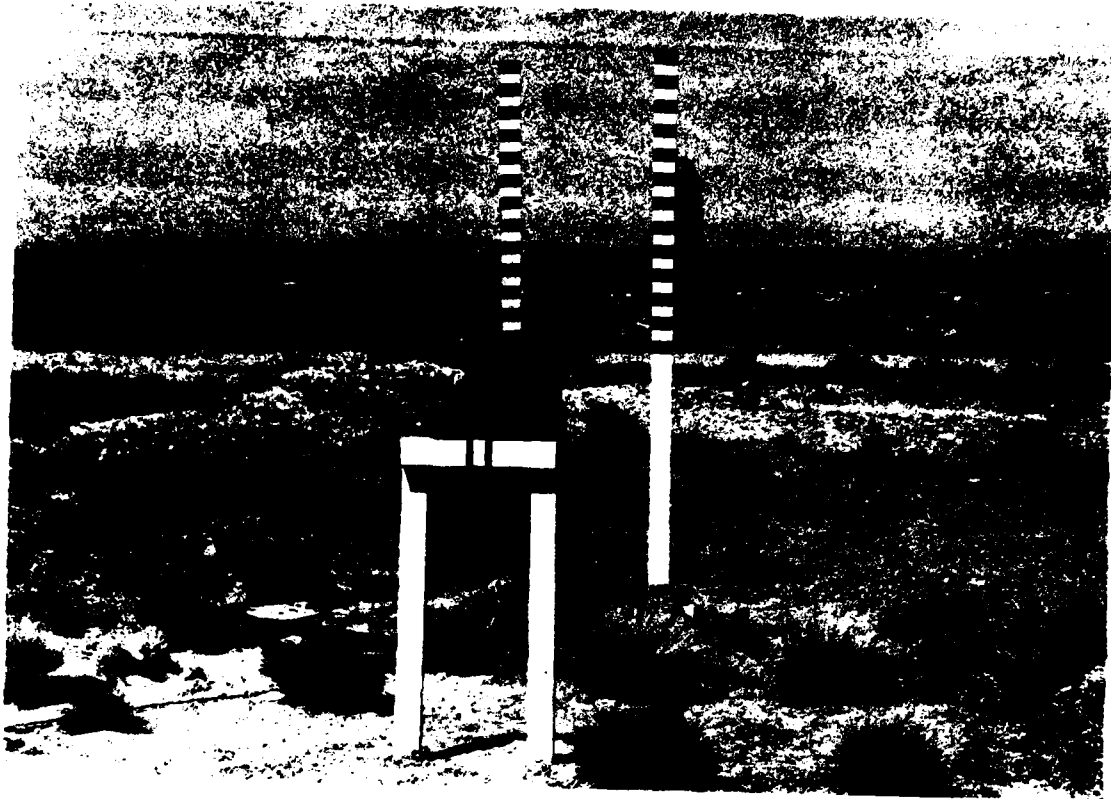


Figure 6. Launch tube.

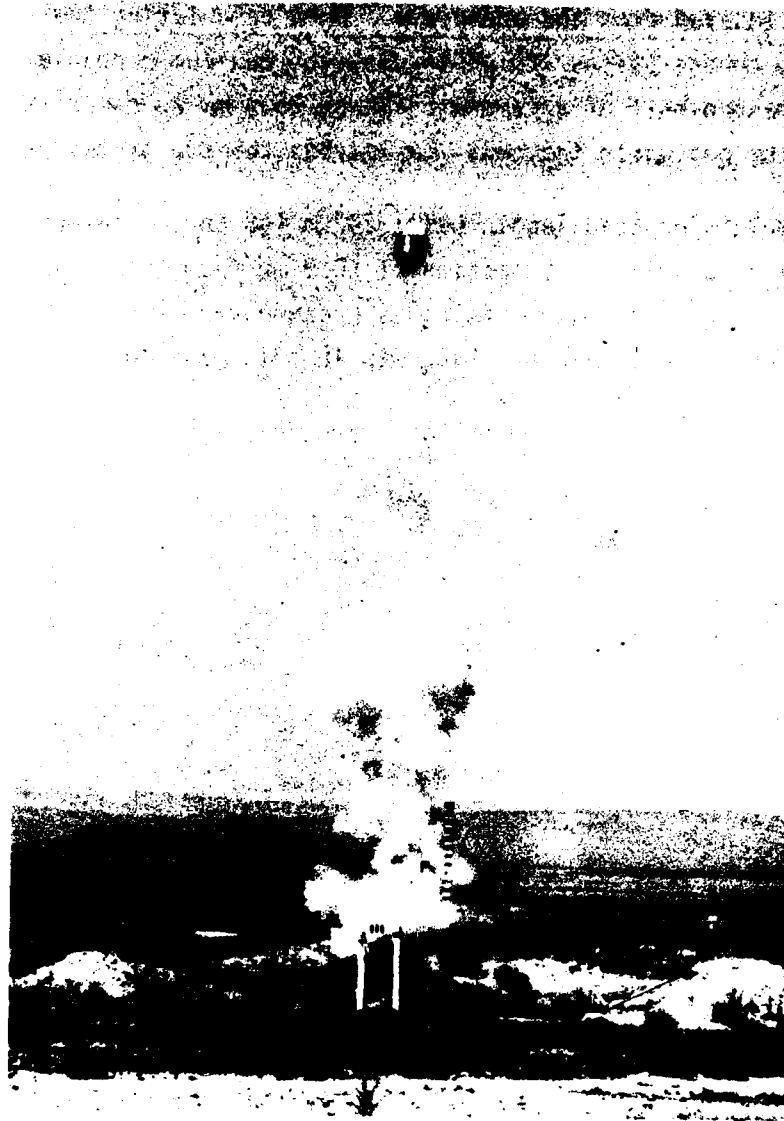


Figure 7. Explosively propelled sphere.

the camera was located from the photopole. When calculating the average velocity as the sphere passes the photopole, the maximum probable inaccuracy is assumed to be one-half of a camera frame or 25.4 mm as the sphere enters the bottom of the photopole and ± 25.4 mm leaving the top of the photopole.

The photopole's exposed length was 1.292 m (48 in). The worst assumed condition for accuracy is a subtraction of 50.8 mm from the nominal length of the photopole. The error in the timing is presumed to be plus or minus the shutter open time for the camera, which was in this case 400 μ s.

Thus the total decimal error may be expressed as

$$\frac{\Delta V}{V} = \frac{\Delta x}{x} - \frac{\Delta t}{t}$$

which is 0.037 or 3.7 percent.

VI. TIME-OF-FLIGHT AND VELOCITY EQUATIONS

Up until now the subject of drag has not been treated. The travel of geometric bodies through air is obviously affected by the air. If they were not, sky-diving would have long ago ceased to be an active sport. In fact, Galileo's original experiment with free-falling bodies, using the Leaning Tower of Pisa, is either only legend or prevarication; it cannot be duplicated. The reason for this is air drag.

Baum (Ref. 1) presents the flight equations studied by Bob Golabic of RAD, Inc, in Colorado Springs. The following, including Figure 8, are excerpts from Reference 1:

For the case going up,

$$ma = -D - W \quad (1)$$

or

$$m \frac{dV}{dt} = -C_D A \frac{1}{2} \rho V^2 - W \text{ (considering drag)} \quad (2)$$

where m = mass

C_D = drag coefficient

ρ = air density

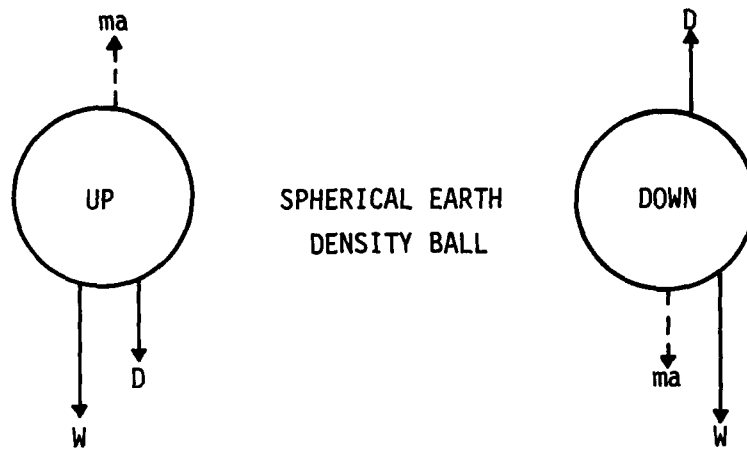
A = cross-sectional area of sphere

W = weight of sphere

Equation 2 may be rewritten as

$$\frac{1}{g} \frac{dV}{dt} = \left(\frac{\rho C_D A}{2W} \right) V^2 - 1 \quad (3)$$

1. Baum, Neal, *BLEST Impulse Gage Development*, AFWL-TR-80-13, Air Force Weapons Laboratory, Kirtland Air Force Base, New Mexico, October 1980.



D = drag
W = weight
ma = mass x acceleration

Figure 8. Forces acting on vertically launched ball.

or

$$\int_{V_0}^V \frac{dV}{\frac{\rho C_D A}{2W} V^2 + 1} = - \int_0^t g dt \quad (4)$$

where V_0 is the launch velocity. If one defines C_0 as

$$C_0 = \frac{\rho C_D A}{2Wg} = \frac{3C_D \rho}{8\rho_s g r} \quad (5)$$

and

$$C_1 = \text{arc tan } (V_0 C_0) \quad (6)$$

then, assuming a constant drag coefficient,

$$-gt = \frac{1}{C_0} [\text{arc tan } (V_0 C_0 - C_1)] \quad (7)$$

To determine the total ascent time (T_u), it is noted that $V \rightarrow 0$. Thus,

$$t_u = \frac{C_1}{C_0 g} = \frac{1}{g C_0} \text{arc tan } (V_0 C_0) \quad (8)$$

To determine the descent time (t_d), the peak height (Z) of the ascent must be determined. Thus, rearranging Equation 7, it can be shown that

$$\frac{dx}{dt} = \frac{1}{C_0} \tan (C_1 - C_0 g t) \quad (9)$$

or, when integrating the right side between 0 and t_u

$$Z = - \frac{1}{C_0^2 g} \ln (\cos C_1) \quad (10)$$

Now, in the case of a downward trajectory

$$ma = -D + W \quad (11)$$

or

$$\frac{dV}{1 - C_0^2 V^2} = g dt \quad (12)$$

if

$$k = \frac{1}{C_0} \quad (13)$$

then

$$\int_0^V \frac{k^2 dV}{k^2 - V^2} = \int_0^t g dt \quad (14)$$

or

$$V = \frac{dx}{dt} = k \left(\frac{e^{\frac{2gt}{k}} - 1}{1 + e^{\frac{2gt}{k}}} \right) \quad (15)$$

This equation may be rewritten in the form

$$\int_0^Z dx = k \int_0^{t_d} \tan h \left(\frac{gt}{k} \right) dt \quad (16)$$

or

$$Z = \frac{1}{C_0^2 g} \ln \left[\cosh \left(C_0 g t_d \right) \right] \quad (17)$$

Returning to Equation 10 and substituting the value of Z, one finds that

$$t_d = \frac{1}{g C_0} \operatorname{arc} \cos h \left(\left(\cos \left[\operatorname{arc} \tan (V_0 C_0) \right] \right)^{-1} \right) \quad (18)$$

The equation for the no-drag case is $t = \frac{2V_0}{g}$ where $t =$ total flight time $t_u + t_d$.

Appendix A shows a sample calculation computing time of flight and velocity (Ref. 2). Table A-1 in the appendix lists time of flight versus launch velocity for an earth density sphere. Figure 9 is a graphical plot of time of flight versus launch velocity with atmospheric drag.

2. Horner, I. B., *Fluid Dynamic Drag*, published by the author, 1958.

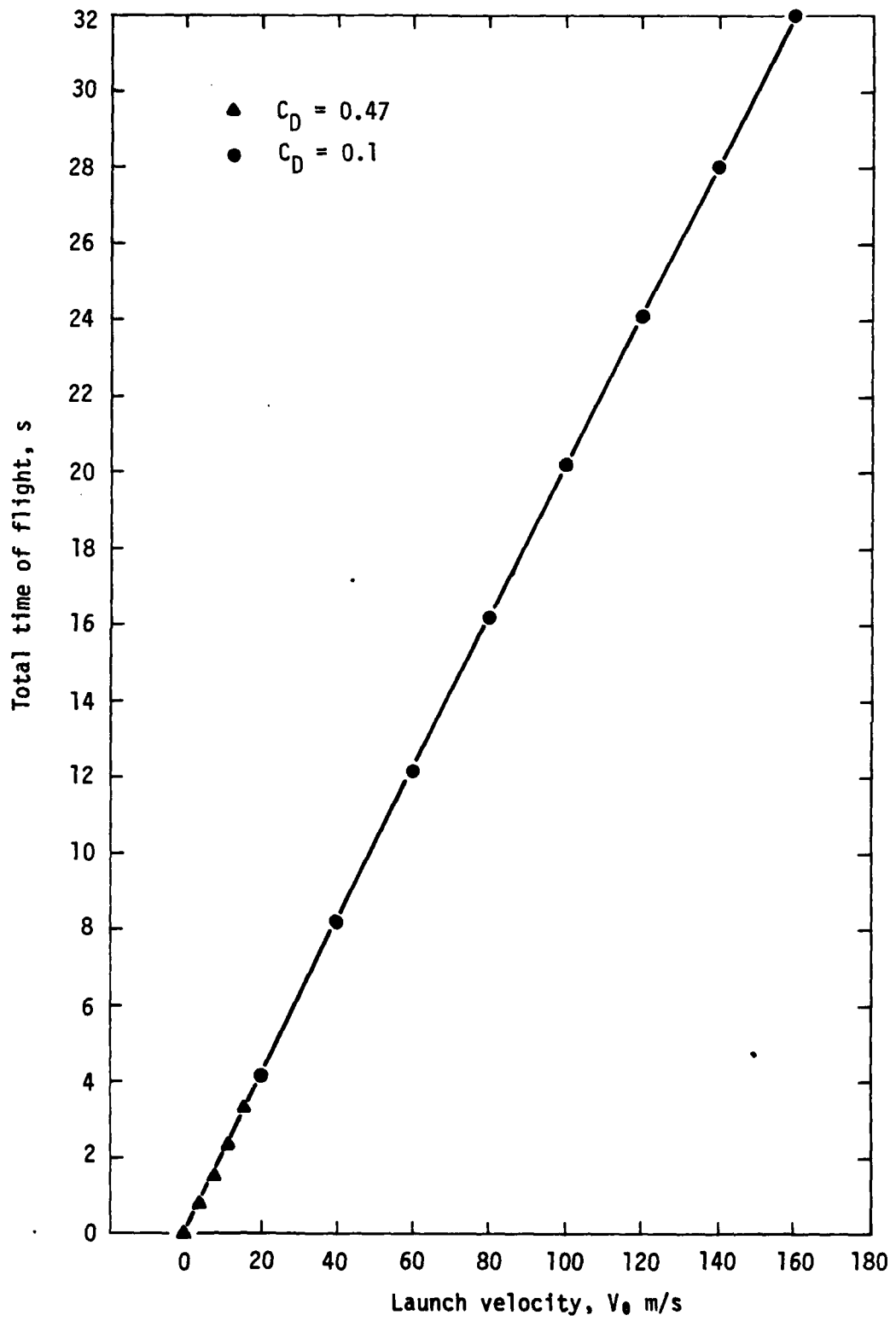


Figure 9. Time of flight versus launch velocity with drag.

VII. CONCLUSION AND RECOMMENDATIONS

The first conclusion has to do with accuracy. The experiments in launching the sphere indicated that the velocity inferred from the time of flight was accurate to 3.6 percent. This is somewhat difficult to interpret because the accuracy of the velocity measurement (photographic) was only 3.7 percent. The time of flight was at least as accurate as the standard used to measure it.

Other measurements were made using the timer only and not the sphere*. These were done on a shaped HEST, part of a test called HYBD-1 (21). These measurements are summarized in Table 1 from Reference 3. Here the average agreement with the time-of-flight and other measurements of impulse is 2.8 percent. This is better than the normal measurements of pressure, acceleration, and photopoles.

TABLE 1. TOTAL IMPULSE AS A FUNCTION OF MEASUREMENT TYPE AND ZONE OF THE SHAPED HEST

Measurement type	Total Impulse, MPa-s			
	Time of Flight	Pressure	Acceleration	Photopole
Zone 8	0.0135	0.0136	0.0134	0.0136
Zone 5	0.0126	0.01245	0.0129	---
Zone 6	0.0108	0.0119	---	---

(Ref. 3)

The theoretical accuracy of the device can be simply determined from the accuracy of the timer. This is ± 0.01 s. For an average time of flight (7 s), the accuracy in velocity is 0.14 percent. This presumes that all the constants used in correcting the drag are correct. This is obviously not true.

3. Palmer, D. G., *HYBD-1 (21) Final Data Report*, NMERI TA9-14, Air Force Weapons Laboratory, Kirtland Air Force Base, NM, December 1981.

*While it is noted that air drag is a minimal effect at these velocities, the author still recommends the use of a sphere. This is for the simple reason that the drag effects on a sphere are known.

The conclusion is that the instrument being tested is more accurate than the standards used to test it. Since the worst velocity inaccuracy observed was of the order of 4 percent, it can be stated that the time-of-flight measurement of the velocity is at least this accurate. Thus Figure 9 may be used by the experimenter to determine launch velocity.

Table 1 also indicates another advantage of the time-of-flight gage. The reason some of the measurements were not given is because of failure. In the case of the photopoles, failure resulted from obscuration. In the case of acceleration, cable failure was the cause. There were no failures in time-of-flight measurements. Thus Table 1 indicates relative reliability as well as accuracy.

The accuracy, reliability, and ease of installation indicate to the author that the time-of-flight gage should be used in all tests where appropriate. This includes both BLEST and HEST.

APPENDIX A
TIME-OF-FLIGHT AND VELOCITY SAMPLE CALCULATIONS

Determine drag coefficient, C_D , from 1 m/s to 160 m/s. Calculate Reynolds number, R , from 1 m/s to 160 m/s using information from Reference 2.

$$R = \frac{Vl}{\sqrt{\nu}}$$

where

V = ft/s, velocity

l = body length, 1 ft

$\sqrt{\nu}$ = kinetic viscosity = 1.56×10^{-4} ft²/s

Table A-1 from Reference 2 shows a constant $C_D = 0.47$ between $R = 10^3$ and 4×10^5 . At 4×10^5 , C_D drops to 0.1 and remains constant beyond 10^6 .

Determine velocity at which $R = 4 \times 10^5$ is the crossover point from $C_D = 0.47$ to $C_D = 0.1$.

$$R = \frac{Vl}{\sqrt{\nu}}, \quad V = \frac{R\sqrt{\nu}}{l}$$

$$V = (400,000) (0.000156) = 62.4 \text{ ft/s}$$

$$\text{or} = 19.02 \text{ m/s}$$

$R/R_{\text{sea level}} = 0.9$ and velocity is directly proportional to R . The crossover velocity is $V = (0.9)(19.02) = 17 \text{ m/s}$ at 5000-ft altitude. Therefore, $C_D = 0.47$ should be used for all velocities less than 17 m/s and $C_D = 0.1$ for all velocities greater than 17 m/s.

The following is a sample calculation determining time up, t_u , time down, t_d , and total time of flight for velocity $V_0 = 100 \text{ m/s}$ taking drag into account.

TABLE A-1. TIME-OF-FLIGHT VERSUS LAUNCH VELOCITY FOR EARTH DENSITY SPHERES

Drag coefficient, C_D	Sphere liftoff velocity, V_0 m/s	t_{up}	t_{down}	Total t_{drag}	Total $t_{no-drag}$	% difference t_{drag} versus $t_{no-drag}$
0.47	4	0.41	0.56	0.97	0.82	15.46
0.47	8	0.82	0.79	1.61	1.63	1.24
0.47	12	1.22	1.25	2.47	2.45	0.81
0.47	16	1.63	1.67	3.30	3.27	0.91
0.1	20	2.04	2.04	4.08	4.08	0
0.1	40	4.08	4.08	8.16	8.16	0
0.1	60	6.10	6.11	12.21	12.24	0.25
0.1	80	8.11	8.14	16.25	16.33	0.49
0.1	100	10.10	10.16	20.26	20.41	0.73
0.1	120	12.00	12.08	24.08	24.49	1.70
0.1	140	13.96	14.10	28.06	28.57	1.82
0.1	160	15.86	16.06	31.92	32.65	2.29

Note: Values in seconds except where indicated.

Air density, $\rho = 1.22 \text{ kg/m}^3$

Soil density, $\rho_s = 1760 \text{ ks/m}^3$

Gravitational acceleration, $g = 9.8 \text{ m/s}^2$

$t = t_u + t_d$ (time up and time down)

Sphere radius, $r = 0.1524 \text{ m}$ (6 in)

$$t_{no-drag} = \frac{2V_0}{g}$$

From Table A-1, where

$$V_0 = 100 \text{ m/s}$$

air density	$\rho = 1.22 \text{ kg/m}^3$
soil density	$\rho_s = 1760 \text{ kg/m}^3$
gravitational acceleration	$g = 9.8 \text{ m/s}^2$
sphere radius	$r = 0.1524 \text{ m (6 in)}$

$$C_D = \frac{3C_{D0}}{8 \frac{\rho}{\rho_s} g r} = \frac{(3)(0.1)(1.22)}{(8)(1760)(9.8)(0.1524)} = 0.0017405$$

Time up, $t_u = 1/gC_D \arctan(V_0 C_D)$ from Equation 8.

$$t_u = \frac{1}{(9.8)(0.0017405)} \arctan [(100)(0.0017405)]$$

$$t_u = (58.6273)(0.1723237) = 10.102876 \text{ s}$$

Time down, $t_d = 1/gC_D \operatorname{arcosh} \left[\frac{1}{\cos [\arctan(V_0 C_D)]} \right]$ from Equation 18.

$$t_d = \frac{1}{(9.8)(0.0017405)} \operatorname{arcosh} (1.0150337)$$

$$t_d = 58.673 \operatorname{arcosh} 1.0150337$$

$$\operatorname{cosh}^{-1} 1.0150337 = 0.173183$$

$$t_d = (58.673)(0.173183) = 10.161168 \text{ s}$$

Total flight time, $t = t_u + t_d = 10.10 + 10.16 = 20.26 \text{ s}$

For the no-drag case, the total flight time is $t = 2V_0/g = (2)(100)/9.8 = 20.41 \text{ s}$.

If the no-drag total flight time equalled the drag case total flight time, the takeoff velocity V_0 would be

$$V_0 = \frac{tg}{2} = \frac{(20.26)(9.8)}{2} = 99.274 \text{ m/s}$$

The percent error using the no-drag case versus the drag case would be

$$\text{error} = \frac{100 - 99.274}{100} \times 100 = 0.726 \text{ percent}$$

**DAT
FILM**

8 —